Spectral Absorption of Solar Radiation in Cloudy Atmospheres: A 20 cm^{-1} Model

ROGER DAVIES, WILLIAM L. RIDGWAY AND KYUNG-EAK KIM[1]

Department of Geosciences, Purdue University, West Lafayette, IN 47907

(Manuscript received 2 February 1984, in final form 8 May 1984)

ABSTRACT

The spectral absorption of solar radiation in typical water clouds is determined using a radiative transfer model based on LOWTRAN transmission functions at a 20 cm^{-1} resolution and Monte Carlo simulations of photon pathlength distributions. Relative absorption by the vapor and droplets within each cloud is obtained, and both plane-parallel and horizontally finite clouds are considered.

Results indicate slightly lower absorption than found previously, with boundary layer clouds typically absorbing 9% of the extraterrestrial insolation for overhead sun. Cloud absorption depends strongly on the presence of water vapor above the cloud top and solar zenith angle, moderately on cloud aspect ratio, and (provided the cloud is neither tenuous nor broken) weakly on cloud type and thickness. The droplets, not the vapor, are shown to be the dominant absorbers within the cloud, except in the absence of water vapor above the cloud top, in which case the vapor and droplets make similar contributions to the total cloud absorption. For many of the cases modeled, the sum of the cloud and atmospheric absorption remained invariant, allowing the net solar radiation budget at the surface to be deduced from broadband satellite measurements of albedo. An explanation for this behavior is found in the analysis of the spectral absorption by the different components.

1. Introduction

Clouds appear to absorb up to 20% of the solar energy incident on them, with solar heating rates reaching over 2 K h^{-1} near cloud tops (Slingo and Schrecker, 1982). This absorption is important for a number of reasons: The total cloud absorption is a major component of the atmospheric radiation budget, affecting climate; local solar heating rates become very strong near sunlit cloud surfaces, affecting cloud development through interactions with droplet evolution; and the spectral absorption of solar radiation strongly modulates the reflection and transmission of solar radiances scattered by the cloud, potentially enhancing the remote sensing of cloud properties.

The above numbers are not definitive, however, and our understanding of cloud absorption remains limited from both observational and theoretical perspectives. One recent radiation text (Liou, 1980, p. 328), for example, suggests that clouds absorb 4% of the global insolation, whereas another (Paltridge and Platt, 1976, p. 8) suggests 11% for the same quantity. For climate modeling purposes, this uncertainty exceeds the change in the earth's radiation budget due to a doubling of atmospheric CO_2 content or a 2% change in the solar output.

The observational evidence of cloud absorption has been largely limited to the measurements of one-dimensional flux divergence using broadband pyranometers. An elementary error analysis of this technique shows that even under optimal conditions of horizontally homogeneous cloud with well calibrated sensors making simultaneous measurements at cloud top and cloud base, such a technique is best suited to determining the upper limit of cloud absorption. The spectral measurement of cloud reflectivity, (see, e.g., Twomey and Cocks, 1982), offers a promising indirect approach to the problem, as does the technique of measuring the internal radiance field suggested by King (1981). Until these new techniques have been widely applied, however, it appears that our understanding of cloud absorption will remain dependent on theoretical modeling. This is especially true if we seek the dependence of cloud absorption on the major meteorological variables that may affect it, such as cloud type and amount, solar zenith angle, atmospheric water vapor amount, etc., or if we seek to understand the relative importance of cloud droplets and cloud water vapor in the absorption process. A knowledge of these dependences is particularly relevant to climate modeling.

The problem of modeling the transfer of solar radiation in clouds across broad spectral intervals can be separated into two components. The first involves the treatment of multiple scattering by the cloud droplets, which should be capable of including such features as one- to three-dimensional cloud inhomo-

[1] Present affiliation: Desert Research Institute, University of Nevada System, Reno, NV 89506.

geneities, and which is usually done on a monochromatic basis. The second relates to the treatment of the rapid spectral variation of water vapor transmission, which may vary on a spectral scale of less than 0.1 cm^{-1}, creating difficulties for the general application of a series of equivalent monochromatic formalisms, as in the use of the *k*-distribution (Lacis and Hansen, 1974) or exponential sum fits (Wiscombe and Evans, 1977). The second component is further complicated by spectral variability in the droplet absorption within the vapor absorption bands. The computational requirements of modeling the multiple scattering by cloud droplets, while at the same time accounting for vapor transmission within and above the cloud, are such that the complete problem has been largely avoided.

In evaluating the relative importance of cloud droplets and cloud vapor on absorption, for example, shortcuts have characteristically been made, whereby the problem has been tackled with and without vapor absorption and the difference attributed solely to water vapor. This approach is valid only if the droplet and vapor absorption occur in entirely separable spectral regions. Since a fair amount of droplet and vapor absorption takes place in the same spectral regions, however, this shortcut is of dubious accuracy, and tends to underestimate the vapor absorption by an unknown amount. As greater spectral resolution has been used in recent models, we find that our understanding of the relative importance of droplet absorption has changed considerably: Paltridge and Platt (1976, p. 104) stated that "liquid absorption is certainly small"; Stephens (1978) used exponential sum fits, together with adding–doubling, in a study which concluded that the absorption of solar radiation by liquid water and by water vapor in clouds is equally significant, except for thin clouds in which water vapor absorption dominates; Welch and Cox (1980) used a similar technique and reached similar conclusions for thick clouds, but found droplet absorption dominant in thin clouds; finally, Slingo and Schrecker (1982) applied exponential sum fits at higher resolution, coupled with delta-Eddington, in a study which concluded that water vapor absorption could be neglected in boundary-layer clouds.

Here we study the relative absorption by cloud droplets and cloud vapor, as well as the general dependence of spectral cloud absorption on the meteorological variables. In so doing, a model is developed which accounts in detail for multiple scattering and absorption by the droplets, as well as for water vapor transmission within and, most importantly, above the cloud. The model first makes use of standard Mie calculations, integrated over typical droplet size distributions, to obtain the spectral properties of the cloud droplets. Monte Carlo simulation is then used to generate pathlength distributions for photons emerging from a variety of conservative clouds. Water vapor transmission is obtained using LOWTRAN 5 (Kneizys *et al.*, 1980) as modified by Robertson *et al.* (1981), and the spectral absorption by both cloud liquid and cloud vapor is finally obtained by an appropriate integration over pathlength. The results generated by this model are then analyzed to determine their chief dependences on the meteorological input variables.

The cloud droplet properties are assumed to be those of spherical drops of pure water with a homogeneous size distribution within the cloud. The water vapor density within the cloud is calculated assuming 100% relative humidity, and is scaled to the mean cloud pressure and temperature for use in the LOWTRAN transmission functions. The effects of internal cloud inhomogeneities, variable pressure scaling of water vapor within the cloud (relevant only for vertically extensive clouds), ice phase absorption, and any potential aerosol absorption, are thus ignored here in order to limit the scope of the problem addressed. Other effects such as Rayleigh scattering, and reflection by an underlying surface of radiation transmitted through the cloud, occur primarily at wavelengths shorter than those of relevance here, and consequently need not be considered.

2. Spectral characteristics of water vapor and cloud droplets

The spectral properties of cloud droplets and water vapor have recently been discussed by Slingo and Schrecker (1982) and Kneizys *et al.* (1980), respectively, so that only a brief summary is given here.

The volume scattering coefficients, asymmetry factors and volume absorption coefficients characteristic of three cloud types were calculated using refractive index data for water given by Hale and Querry (1973), modified gamma drop-size distributions quoted by Welch and Cox (1980), as summarized in Table 1, and the Mie code of Wiscombe (1979). Figure 1 shows the results of these calculations as functions of wavenumber. Except for a region of strong absorption for wavenumbers less than 4000 cm^{-1}, the spectral dependence of both the scattering coefficient and the asymmetry factor is slight. The variability with cloud type totally masks the spectral dependence in the case of the scattering coefficient, and is roughly equivalent in magnitude to the range of the asymmetry factor from 4000 to 15 000 cm^{-1}. Also, because of the strong droplet absorption in the spectral region below 4000 cm^{-1}, the spectrally integrated cloud absorption, and to a large extent the spectral cloud absorption, is insensitive to the details of the asymmetry factor and the scattering coefficient in this region. In the following model development, therefore, we take both the asymmetry factor and the scattering coefficient for each cloud type to be spectrally invariant. Single-scatter albedo, on the other

TABLE 1. Summary of droplet properties used.

Cloud type	Modal radius (μm)	Liquid water (g m^{-3})	Droplet concentration (cm^{-3})	Scattering coefficient (visible) (km^{-1})	Asymmetry factor (visible)
Stratocumulus	5.33	0.141	100	28	0.86
Stratus	6.75	0.379	100	54	0.86
Nimbostratus	9.67	1.034	100	100	0.86

hand, varies substantially with wavenumber, and is included in our model at a spectral resolution of typically 100 cm^{-1}.

Transmission through water vapor varies very rapidly with wavenumber, so that when averaged over even a few cm^{-1} the transmission function quickly becomes nonexponential with pathlength or amount. This does not matter in our model, however, as the pathlength distributions described below do not require an equivalent monochromatic formalism, and may utilize transmission functions of arbitrary shape. The best currently available treatment of water vapor at moderate resolution appears to be that of LOWTRAN 5 (Kneizys *et al.*, 1980) or a modified version of LOWTRAN called BMOD (Robertson *et al.*, 1981).

LOWTRAN uses a single parameter scaling of tabulated spectral data based on transmission measurements and degraded high resolution models to produce transmission functions at 20 cm^{-1} resolution. The water vapor transmission functions are functions of the scaled water vapor amount w, given by

$$w = \frac{1}{\rho_w}\int_0^l \rho_v\left[\frac{p}{p_0}\left(\frac{T_0}{T}\right)^{1/2}\right]^{0.9} dl', \qquad (1)$$

where ρ_v is the actual vapor density, ρ_w the liquid water density, l the physical path length, p_0 the standard pressure (1 atm) and T_0 the standard temperature (273.15 K).

BMOD is a 5 cm^{-1} resolution band model which uses multiple-parameter scaling and the Curtis–Godson approximation for inhomogeneous paths, accounting for the single line contributions to the spectral transmittance in a statistical fashion. In order to use BMOD in our model with single parameter vapor transmission functions, we first reduce inhomogeneous vapor paths to their equivalent amount at 2 km altitude using Eq. (1).

Although based on different spectral models, the two versions appear to be quite similar for our purposes (after BMOD is degraded to 20 cm^{-1}), as is shown from the comparative transmissions at a spectral resolution of 20 cm^{-1} through a horizontal 1 cm water vapor path at STP in Fig. 2. The largest differences occur around 9000 cm^{-1} and cause some uncertainty in the subsequent spectral cloud absorption in this region, as discussed later. The accuracy of these transmission functions when applied to broad spectral intervals does not appear to have been examined experimentally, however, and this may well be one of the limitations of our model. Should these values be improved in the future, their subsequent incorporation in a model such as ours would be an easy task.

The ultimate spectral resolution of our model is therefore determined by the resolution of the water vapor transmission functions utilized. The highest resolution available from LOWTRAN is 20 cm^{-1}, which is used in some of our results below. A coarser resolution is appropriate for spectral averages, since the transmission functions may first be averaged over an interval as broad as that allowed by variations in the solar spectrum and the droplet absorption coefficient. A resolution of 100 cm^{-1} was adopted for this purpose.

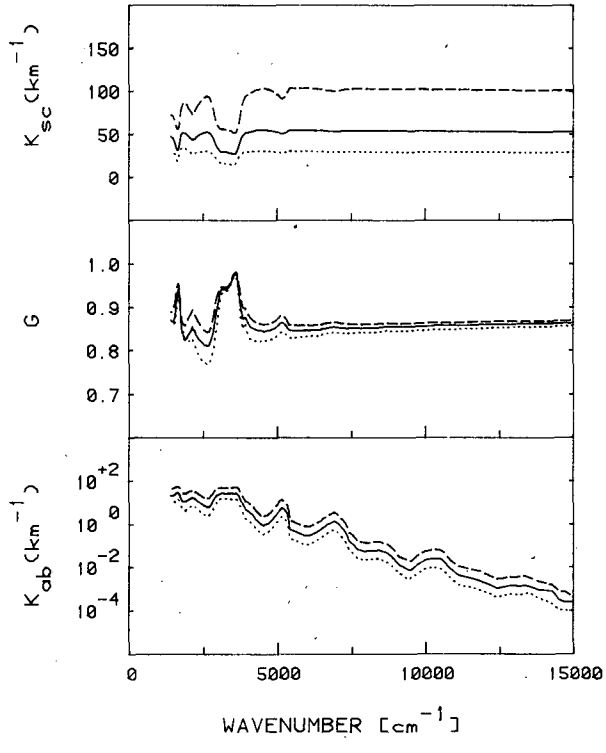

FIG. 1. The spectral dependence of typical droplet properties for stratus (solid), stratocumulus (dotted) and nimbostratus (dashed). Top panel, volume scattering coefficient; middle panel, asymmetry factor; bottom panel, volume absorption coefficient.

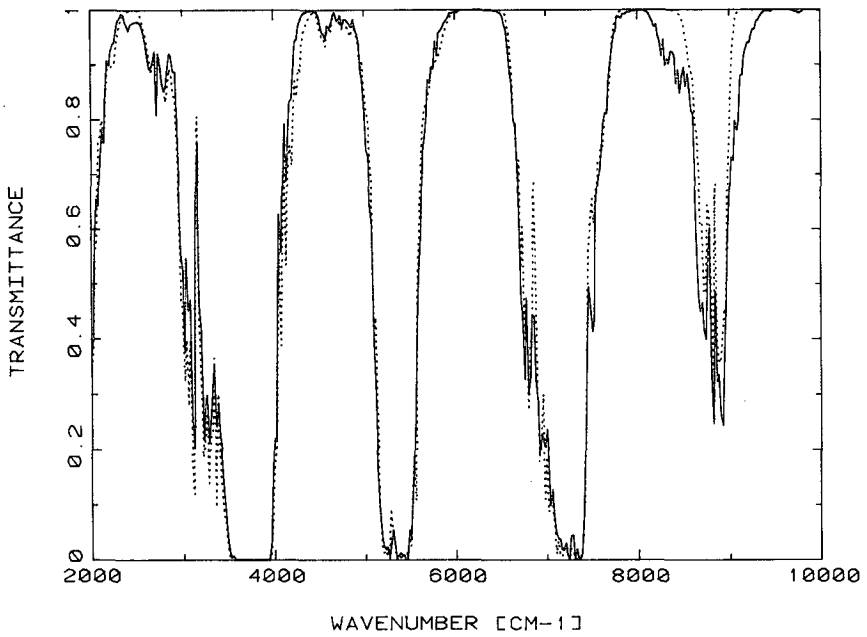

FIG. 2. Spectral water vapor transmission at 20 cm^{-1} resolution through a 1 cm sea-level path of water vapor, using BMOD (solid) and LOWTRAN 5 (dotted).

3. Model development

Photon pathlength distributions have been used to study radiative transfer in scattering and absorbing media by, among others, Irvine (1964), Kargin *et al.* (1972) and Appleby and Irvine (1973). Van de Hulst (1980, Ch. 17) has recently reviewed this field. Our model differs from these mainly in the details that are relevant to its present application. We thus make use of the equivalence theorem of van de Hulst (1980, p. 574), by which a cloud of absorbing vapor plus absorbing and scattering droplets is radiatively equivalent to a cloud of purely scattering droplets embedded in a distributed absorbing medium. The scattering characteristics of the cloud are therefore fully described for our purposes by the distribution of pathlengths of emerging photons from an equivalent conservative cloud with the same scattering optical thickness. The effects of absorption are then included by convolution over pathlength of this distribution with the total transmission function through an equivalent non-scattering medium of vapor and absorbing droplets.

The model thus has a number of stages to its implementation. Mie calculations are first integrated over the droplet size distribution to obtain the droplet characteristics for each relevant spectral subinterval. Pathlength distributions are then generated for each equivalent conservative cloud (and solar zenith angle). This is done using the Monte Carlo model of Davies (1978), which is extended to include summaries of the photon pathlengths. Finally, the total transmission function through vapor and droplets, obtained from the Mie absorption coefficients and LOWTRAN, is integrated over the pathlength distribution for each spectral subinterval.

More explicitly, the total cloud absorption for a spectral subinterval $[\nu - \Delta\nu/2, \nu + \Delta\nu/2]$ is given by

$$A(\nu, \Delta\nu) = F_\nu \int_0^\infty p(l)\{T(\nu, \Delta\nu, y_0) - T[\nu, \Delta\nu, y_0 + y(l)] \exp(-k_\nu l)\}dl, \quad (2)$$

where

ν	wavenumber at the center of the subinterval,
$\Delta\nu$	width of the subinterval in wavenumbers,
F_ν	extraterrestrial spectral insolation, from Thekaekara and Drummond (1971), depleted by the nonvapor extinction above the cloud top,
$p(l)dl$	fraction of photons with pathlengths between l and $l + dl$ emerging from an equivalent conservative cloud with the same scattering optical thickness, determined from Monte Carlo simulation,
$T(\nu, \Delta\nu, y)$	transmission through water vapor only of total scaled amount y averaged over subinterval $\Delta\nu$, from LOWTRAN,
y_0	scaled water vapor path down to the cloud top,

$y(l)$ additional scaled water vapor path traversed by a photon of pathlength l within the cloud,

k_ν volume absorption coefficient of droplets at ν, from Mie calculations, integrated over droplet size distribution.

Note that F_ν, $p(l)$ and y_0 each depend on solar zenith angle.

Equation (2) effectively separates the multiple scattering effects, which were shown in the preceding section to be relatively invariant spectrally, from the spectrally varying transmission. The spectral resolution of the cloud absorption from this equation is thus determined by the choice of $\Delta\nu$, which directly affects the water vapor transmission. Of course, as $\Delta\nu$ increases beyond about 100 cm^{-1}, variations in k_ν and F_ν also have an effect. Spectral integration over large intervals therefore proceeds in two steps. The water vapor transmission function is first averaged over the largest $\Delta\nu$ which seems reasonable (up to 100 cm^{-1} for our calculations), and then k_ν and F_ν are allowed to vary in a numerical integration of Eq. (2) with a step size equal to $\Delta\nu$.

Since the droplet absorption coefficient is spectrally uncorrelated with the vapor transmission function over a spectral subinterval of 100 cm^{-1}, the total transmission function of vapor plus droplets is the simple product used in Eq. (2). This allows us to separate the two contributions to total absorption by droplets and vapor as follows. The fractional absorption by water vapor of photons with intermediate path s, where $0 < s < l$, in traversing a path increment Δs is

$$\Delta A'_v = [T(s) - T(s + \Delta s)]e^{-ks} + O(\Delta s^2). \quad (3)$$

The exponential factor in this equation accounts for droplet absorption up to s, and the term of order Δs^2 results from neglect of the effect on the vapor absorption of droplet absorption within the path increment Δs. In the differential limit, we therefore obtain

$$\frac{dA'_v}{ds} = -e^{-ks}\frac{dT}{ds}. \quad (4)$$

This derivative must be integrated over all intermediate paths from zero to l, to give the total absorption by water vapor of photons emerging from the equivalent conservative cloud with pathlength l. Consideration of all photon pathlengths then yields the complete spectral absorption by water vapor within the cloud as

$$A_v(\nu, \Delta\nu) = -F_\nu \int_0^\infty p(l) \int_0^l \exp(-k_\nu s)\frac{dT}{ds}\, dsdl, \quad (5)$$

and the analogous expression for droplet absorption as

$$A_d(\nu, \Delta\nu) = F_\nu \int_0^\infty p(l) \int_0^l T(s)k_\nu \exp(-k_\nu s)dsdl. \quad (6)$$

Note that summation of Eqs. (5) and (6) yields Eq. (2) directly; this redundancy was used in our model as a check on the numerical integration over pathlength, errors in which were less than 0.5%.

4. Spectral results

Our model was applied to a 1 km thick stratus cloud embedded in a 1962 U.S. Standard Atmosphere (McClatchey *et al.*, 1972, Appendix B) with cloud top altitude at 2 km and overhead sun; results are shown in Figs. 3–5. The spectral resolution in Fig. 3 is 20 cm^{-1}; the two absorption curves illustrate the differences between the use of BMOD (solid) and LOWTRAN 5 (dotted). The spectral range of BMOD does not extend beyond 9900 cm^{-1}, so a comparison with LOWTRAN was not possible above this cutoff. There is generally good agreement in the spectral cloud absorption, but discrepancies greater than 10% are evident in the ϕ band of water vapor near 9000 cm^{-1}. The spectrally integrated cloud absorption for this case was found to be 135.3 W m^{-2} using BMOD and 129.2 W m^{-2} using LOWTRAN 5, a difference of about 5%. Most of this difference can be attributed to the different predictions for vapor absorption within the cloud from 8000 to 9500 cm^{-1}.

The importance of including CO_2 in the atmosphere above the cloud top was briefly considered. When the integrated cloud absorption was recalculated with CO_2 removed, it increased by about 4%, and the greatest spectral differences occurred at wavenumbers below 3500 cm^{-1} and near 5000 cm^{-1}. This increase is comparable to the discrepancy between LOWTRAN and BMOD, and so the neglect of CO_2 and the use of LOWTRAN achieves a similar result for the integrated cloud absorption as the use of BMOD and the inclusion of CO_2. This result may be appropriate for some models, since it reduces the computational effort. Such an approximation models the spectral features less precisely, however, so that in all of the following results BMOD has been used and the effects of absorption above the cloud by CO_2 and the other permanent gases have been included. Absorption within the cloud by CO_2 or O_2 has not been modeled, however, because this is relatively small.

The separate components of the spectral cloud absorption of Fig. 3, due to water vapor and cloud droplets, are shown at 50 cm^{-1} resolution in Fig. 4. Most of the sharp spectral behavior is due to the water vapor absorption bands, the relative strength of which (weighted by the solar spectrum) is clearly seen in the dotted curve of column absorption above the cloud. The narrow peak at 13 100 cm^{-1} is due to O_2. The droplet absorption (dashed curve) is largest in the water vapor windows between 4000 and 7000 cm^{-1}, decreasing at larger wavenumbers as the single-scattering albedo approaches unity, while falling off slowly at smaller wavenumbers due to the decreasing

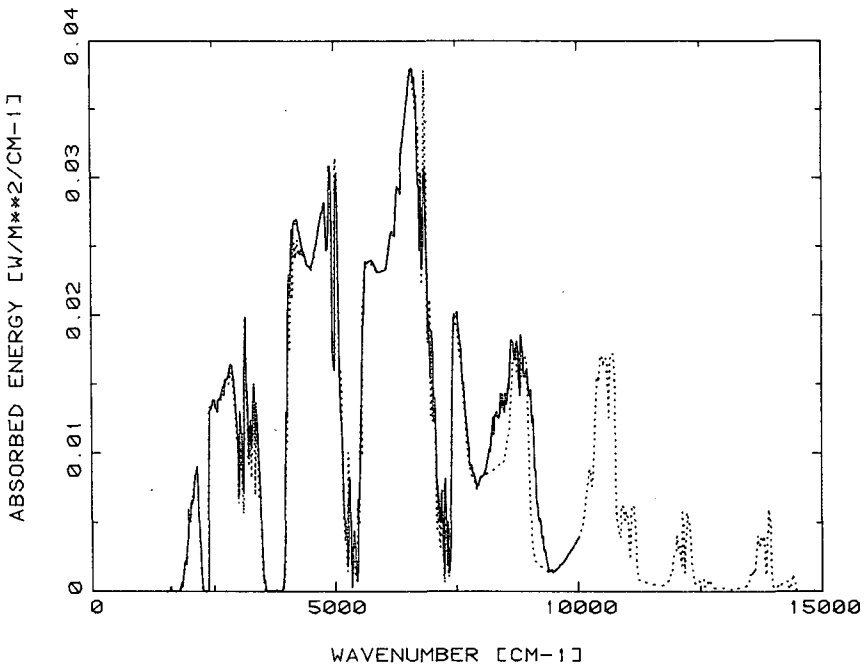

FIG. 3. Spectral absorption at 20 cm^{-1} resolution, typical of a 1 km thick cloud with cloud top altitude of 2 km in a standard atmosphere with overhead sun, using BMOD (solid) and LOWTRAN 5 (dotted).

solar intensity. Vapor absorption within the cloud, depicted by the solid curve of Fig. 4, is seen to be negligible at low wavenumbers, due to strong vapor absorption above the cloud. At larger wavenumbers, however, where the vapor bands are weaker, allowing more radiation to reach the cloud top, and where the droplet absorption is also reduced, the vapor absorption within the cloud may be significant and becomes

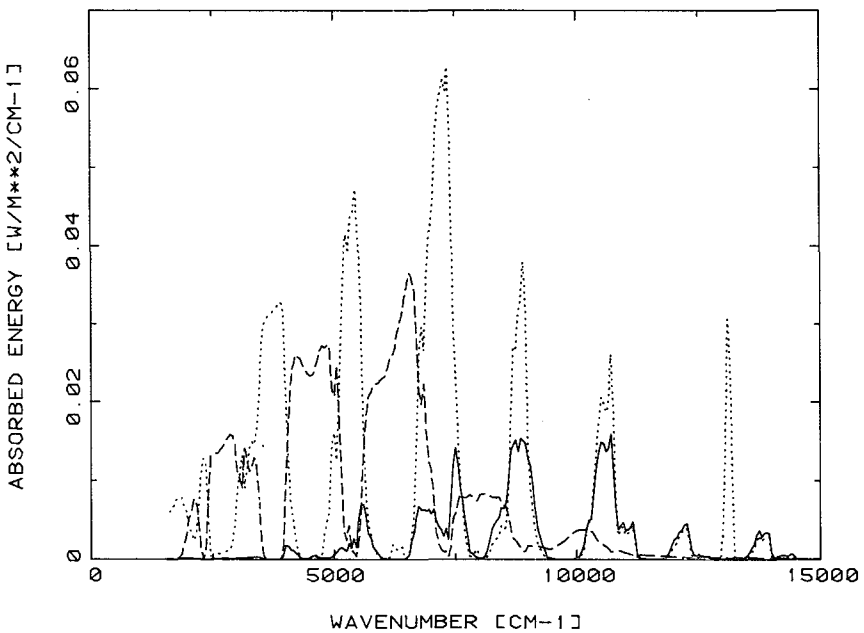

FIG. 4. Spectral absorption at 50 cm^{-1} resolution by cloud water vapor (solid), cloud droplets (dashed) and column vapor (dotted), typical of a 1 km thick stratus cloud with cloud top altitude of 2 km in a standard atmosphere with overhead sun.

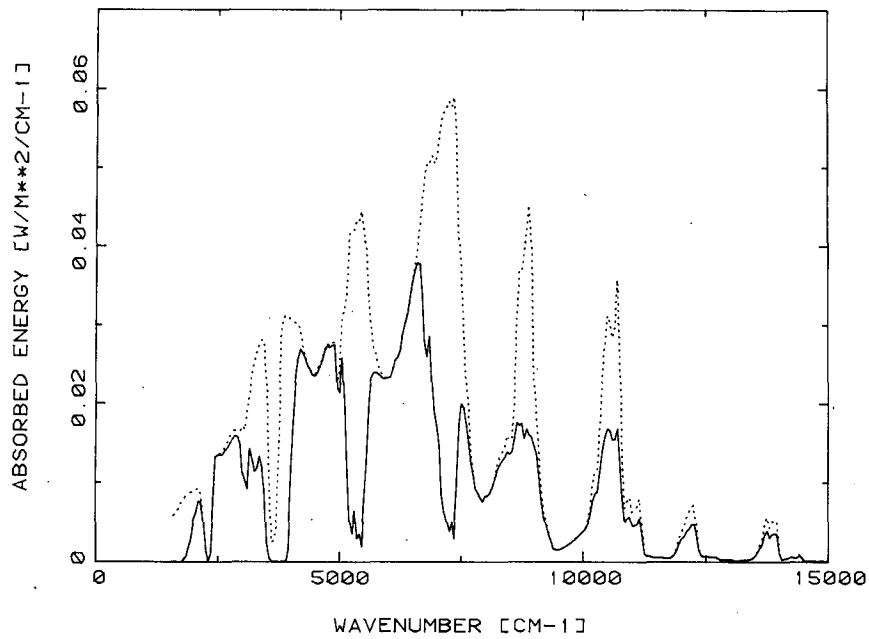

FIG. 5. Spectral cloud absorption at 50 cm^{-1} resolution, typical of a 1 km stratus cloud with cloud top altitude of 2 km and overhead sun. Comparison between the inclusion of water vapor (solid) and its neglect (dotted), in the standard atmosphere above the cloud top.

comparable with the column absorption above the cloud for wavenumbers beyond ~10 000 cm^{-1}. For low wavenumbers, therefore, droplet absorption dominates, whereas cloud vapor is the dominant absorber at high wavenumbers.

The strong effect of column absorption above the cloud top is illustrated in Fig. 5, which contrasts the spectral absorption by the cloud in the standard case (solid) with the absorption that would result if there were no water vapor in the atmosphere above the cloud top (dotted). The previous minima in cloud absorption in the strong vapor absorption bands now become maxima, due to strong absorption by the cloud vapor, and the total cloud absorption more than doubles. Inclusion of atmospheric absorption above the cloud top therefore seems to be an essential part of cloud absorption models.

5. Integrated results

The spectral results of the previous section can be integrated to provide the total absorption for typical clouds with any atmospheric vapor profile and solar zenith angle. As discussed above, we have separated the cloud vapor and droplet contributions to the total absorption in order to better understand how the absorption depends on these factors. We have also calculated the integrated absorption in the atmosphere above the cloud top, including the additional effects of ozone absorption and absorption of radiation reflected by the cloud. While these refinements have a negligible effect on cloud absorption, they are needed to illustrate realistic dependences of total atmospheric absorption on zenith angle and column vapor. The effects of reflected radiation have been calculated assuming that the mean angle of emergence of the reflected photons is $\cos^{-1}(0.6)$. The additional water vapor absorption was calculated, as before, by integrating the LOWTRAN transmission functions over the total photon pathlengths, and the ozone absorption was determined using the Lacis and Hansen (1974) parameterization with a column ozone amount of 0.3 cm STP above the cloud top.

From the spectral results of Figs. 4 and 5, a strong effect due to column vapor absorption above the cloud top can be expected; this is borne out in the integrated absorption values presented in Fig. 6, which shows integrated results for the same stratus cloud case as before, but with variable amounts of column vapor above the cloud. This variation directly simulates changes in the absolute humidity above the cloud, and also illustrates the first-order effects of changing the cloud top altitude (recognizing that there will also be second-order effects due to changes in temperature and pressure).

There is a sharp decrease in the total absorption (dot-dash curve in Fig. 6) with the introduction of modest vapor amounts above the cloud, after which the absorption becomes relatively insensitive to vapor amount. For our standard case of a typical stratus cloud with a cloud top altitude of 2 km in a standard atmosphere with overhead sun, the scaled vapor amount above the cloud top is about 0.4 g cm^{-2} and

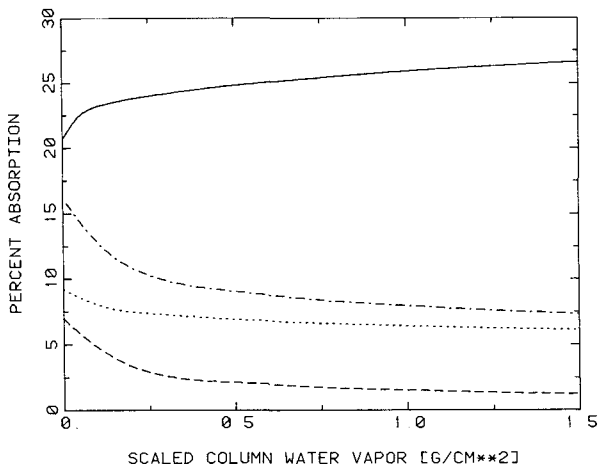

FIG. 6. Integrated absorption, as a percentage of the extraterrestrial insolation, versus scaled water vapor amount above the top of a typical 1 km thick stratus with cloud top altitude of 2 km and overhead sun: Cloud plus above-cloud absorption (solid); total cloud absorption (dot-dash); cloud droplet absorption (dots); cloud vapor absorption (dashed).

the corresponding cloud absorption is 9.4% of the extraterrestrial insolation. Ignoring the column vapor would have yielded an absorption of 16.3%. From a modeling or parameterization perspective, it is therefore essential to include some typical vapor amount above the cloud, but the accuracy of this amount does not appear to be critical.

We also note from Fig. 6 that conclusions as to the relative absorption by cloud droplets (dotted curve) and cloud vapor (dashed curve) depend on whether the vapor above the cloud is ignored, in which case the absorptions are similar, or included, in which case some 75% of the total cloud absorption is typically due to the droplets. Finally, Fig. 6 shows (solid curve) that the amount of vapor above the cloud has little effect on the total atmospheric absorption (that is, the sum of cloud absorption plus column absorption above the cloud), which varies from 21 to 27% over the complete range of vapor amounts, and more typically only from 24 to 26%. Ozone, CO_2 and O_2 in the atmosphere above the cloud top typically absorb about 5% of the extraterrestrial radiation; while this value is independent of water vapor amount above the cloud, it will vary a little with total ozone amount and cloud height.

Another major dependence of integrated cloud absorption is on the solar zenith angle, as illustrated in Fig. 7. Here we see that total cloud absorption (circles) is a maximum for overhead sun and decreases smoothly with increasing zenith angle. This is mainly due to the increase in cloud albedo and, to a lesser extent, the increased vapor path above the cloud. As the solar zenith angle increases, the relative contribution of the droplets (triangles) to total cloud absorption also increases steadily in our standard case from a 75% contribution at overhead sun to an 88% contribution for a solar zenith angle of 80°. Figure 7 also shows that the total atmospheric absorption (crosses) remains remarkably constant at about 25% for zenith angles up to 60°, after which it rises to over 35%. The constancy is largely due to the fact that as more absorption takes place in the water vapor above the cloud there is less absorption within the cloud. The increase above 60° is due chiefly to increased absorption in the Chappuis bands of ozone which cannot be compensated by any reduction in cloud absorption, the cloud already being conservative in this spectral region.

The remaining variables which affect cloud absorption include cloud thickness, liquid water content, homogeneity, temperature, etc.; these may be loosely called the cloud type variables. The effects of finite cloud geometry are considered in the next section; here we present (Fig. 8) the dependence of cloud absorption on the liquid water content of the cloud for the three droplet size distributions given in Table 1. An asymptotic regime is quickly reached for each cloud type as its liquid water content increases, the difference in fractional absorption between cloud types being 0.01 in this limit. Perturbation of the water vapor mixing ratio by a factor of 2 either side of the standard case also yields 0.01 differences in this limit.

As the cloud liquid water content decreases, the total cloud absorption tends to a thin cloud limit due to absorption by the remaining water vapor within the fixed vertical extent of the cloud. Drop-size effects become much reduced in this limit, with perturbations

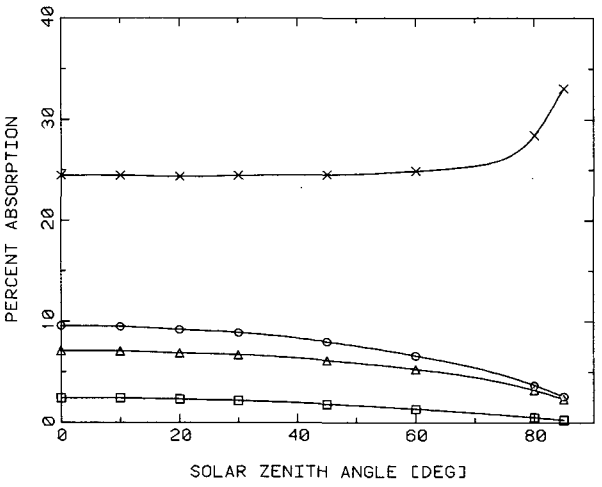

FIG. 7. Integrated absorption, as a percentage of the extraterrestrial insolation, versus solar zenith angle, for a typical 1 km thick stratus with cloud top altitude of 2 km. The curves are cubic spline fits under tension to the individual Monte Carlo results represented by the points, corresponding to cloud vapor absorption (squares), cloud droplet absorption (triangles), total cloud absorption (circles) and total atmospheric absorption (crosses).

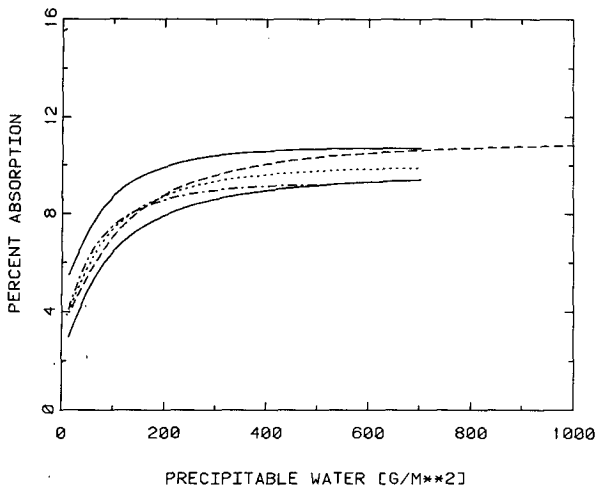

FIG. 8. Integrated cloud absorption, as a percentage of the extraterrestrial insolation, versus liquid water content, for overhead sun and different cloud types between 1 and 2 km in a standard atmosphere: Stratus (dotted); nimbostratus (dashed); stratocumulus (dot-dash); stratus with twice the standard water vapor within the cloud (upper solid); stratus with half the standard water vapor (lower solid).

in water vapor mixing ratio still having a ±0.01 effect. (We have not pursued the thin cloud case to its conclusion by considering absorption below the cloud and possible surface reflection, and so the thin cloud absorptions may be slightly underestimated.)

6. Absorption in finite clouds

The Monte Carlo simulation of photon pathlength distributions can be applied very readily to three-dimensional cloud geometries; a few cases of clouds with finite horizontal extent were considered. Figure 9 shows the nature of the changes to the spectral absorption when the horizontal cloud extent is reduced for fixed vertical extent. The solid curve is the same as in Fig. 5 for the plane-parallel stratus of 1 km thickness, while the other two curves are for horizontal extents of 1 km (dotted) and 0.5 km (dashed). The effect of the cloud sides is such that radiation can diffuse out through the sides before being absorbed within the cloud. While this effect persists at most wavenumbers, there is no appreciable difference in the spectral absorption for regions of strong absorption, such as near 3000 cm^{-1}.

When the spectral absorption in finite clouds is integrated, and the result plotted as a function of aspect ratio (vertical to horizontal extent) for fixed vertical extent (Fig. 10), it can be seen that the total cloud absorption decreases steadily with increasing aspect ratio. This is due to the shorter pathlengths taken by photons in finite clouds, their probability of escape from the cloud increasing as the horizontal cloud extent decreases. As evidenced by the results shown for a 60° solar zenith angle, the relative dependence of absorption on horizontal cloud extent may be reduced at larger zenith angles.

Most clouds have aspect ratios less than one, and

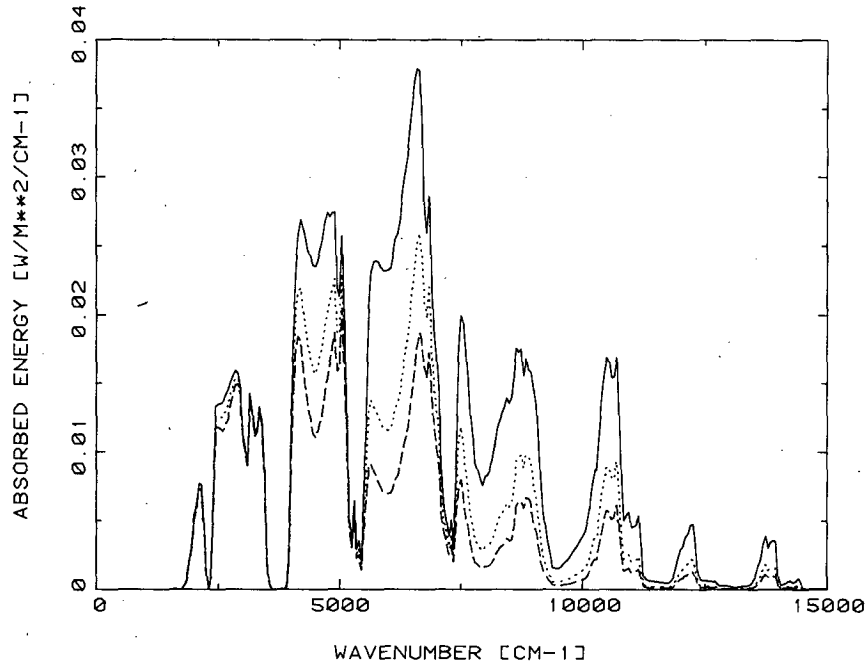

FIG. 9. Spectral absorption at 50 cm^{-1} resolution, typical of 1 km thick stratus with horizontal extents of infinity (solid), 1 km (dotted) and 0.5 km (dashed).

we note from Fig. 10 that even for unit aspect ratio the fractional cloud absorption has decreased by only 0.03. Differences in cloud absorption due to variations in horizontal cloud extent are therefore similar to the differences shown in Fig. 8 due to the other variations in cloud type.

From the results of his monochromatic model, Davies (1978) concluded that one effect of finite geometry is to reduce the broadband albedo at the cloud top, which may give rise to a spurious overestimate of cloud absorption if the cloud is mistakenly thought to be one-dimensional. Inclusion of the integrated effects of real cloud absorption does not substantially alter this conclusion. While real absorption by finite clouds may remain at several percent (e.g., 6%), the escape of photons through the cloud sides will still cause a large (e.g., 30%) reduction in the broadband albedo of finite clouds.

7. Comparison with previous results

In comparing our results with previously reported estimates of cloud absorption, we found some difficulty in obtaining identical input parameters describing the cloud types and atmospheric models, a difficulty also noted by Slingo and Schrecker (1982). Some general agreements and disagreements emerge, however.

We can compare our results fairly directly with those of Welch and Cox (1980) for fractional absorption (in terms of the radiation incident on the cloud top) by their stratus top model cloud in a moist tropical atmosphere, for different cloud top heights (Table 2). Their results are higher than ours, with the difference increasing as the column vapor above the cloud top decreases. These differences may be due to their use of Liou and Sasamori's (1975) empirical water vapor transmission functions, their use of discrete spectral bands, or their apparent use of constant droplet absorption coefficients within the water vapor windows.

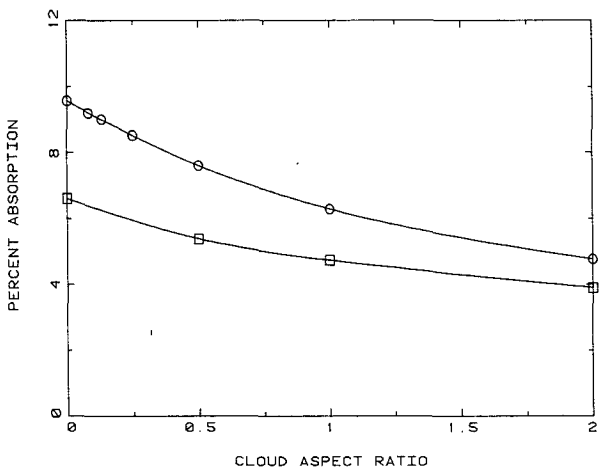

FIG. 10. Integrated absorption, as a percentage of the extraterrestrial insolation intercepted by the cloud, versus aspect ratio, typical of a 1 km stratus cloud, with overhead sun (circles) and a 60° solar zenith angle (squares). The curves are cubic splines under tension, fit to the discrete Monte Carlo points.

TABLE 2. Comparison of results with those of Welch and Cox (1980) for the fractional absorption (with respect to cloud top insolation) by their 1 km thick stratus top model, overhead sun and their GATE III atmosphere (from their Table 2.7).

Cloud top height (km)	This paper	Welch and Cox (1980)
1.5	0.091	0.099
4	0.10	0.12
10	0.13	0.16

A similar difference from Stephens' (1978) results was also obtained for his stratocumulus cloud at 2 km altitude in a standard atmosphere and overhead sun, for which he obtained a fractional absorption of 0.12 (his Table 4). We obtained approximately 0.10 for this case, after matching cloud optical thickness and making approximate allowance for differences in modal radii between the slightly difference cloud models. Our result is consistent with the 25% reduction in the solar heating rate found by Slingo and Schrecker (1982) when comparing their model with Stephens' lower resolution results.

Stephens' conclusion that absorptions of solar radiation by liquid and water vapor within the cloud are equally significant is not borne out by our results, which indicate that liquid water is the dominant absorber, a conclusion also reached by Slingo and Schrecker (1982). Stephens also concluded that the fractional absorption by the cloud is almost independent of cloud height. We find, as did Welch and Cox (1980), that as the cloud height increases, the reduction in column vapor above the cloud top results in a substantially increased fractional absorption by the cloud.

Slingo and Schrecker (1982) provide insufficient detail for an easy comparison with their results, which stress heating rates rather than fractional absorption. We found no significant discrepancies, however, but would qualify their conclusion that water vapor can be neglected with only a small error in boundary layer clouds, by noting that such neglect would typically introduce a 10–30% error in the heating rate, and that this error would increase to 100% if the atmosphere above the cloud were unusually dry.

Liou and Wittman (1979) show fractional cloud absorptions significantly higher than the above results, with a general insensitivity to the atmospheric model used, and a very strong solar zenith angle dependence with a curious turning point for $\theta_0 \approx 80°$. Their subsequent parameterization scheme for cloud absorption does not include any dependence on column

vapor above the cloud top and it is not clear whether this effect was considered.

8. Summary

We have developed a moderate resolution (20 cm^{-1}) model for the spectral absorption of solar radiation in a cloudy atmosphere. Applications of this model are limited here to nonprecipitating clouds with neither ice phase nor major internal inhomogeneities, and the effects of the atmosphere and the surface below the clouds are omitted. The latter effect is normally negligible, but may cause a slight underestimate of absorption by some tenuous or broken clouds. At wavenumbers less than $\sim$7500 cm^{-1}, this model shows that strong absorption by water vapor above the cloud reduces the spectral solar radiation incident on the cloud such that subsequent absorption by the vapor within the cloud is typically negligible. This reduction of spectral insolation also detracts from absorption by the cloud droplets, but since these may also absorb in the water vapor windows, they dominate the cloud absorption in this spectral region.

For increasing wavenumbers greater than $\sim$7500 cm^{-1}, the vapor bands weaken and the imaginary component of the liquid water refractive index decreases, so that the vapor within the cloud becomes progressively more important in determining the spectral absorption. When integrated across the entire spectrum, however, this spectral absorption by the cloud vapor remains a small fraction of the total cloud absorption, which is predominantly due to the cloud droplets.

The above spectral results help to explain the behavior of the spectrally integrated absorption as the input parameters to the model are varied. Much of the total absorption is due to wavenumbers below $\sim$7500 cm^{-1}, where the vapor bands tend to be saturated and there is strong droplet absorption. The total atmospheric absorption in this region tends to be partitioned between cloud droplet absorption and absorption by the vapor above the cloud with a relatively constant sum.

From the comparative results presented above, it appears that our model yields reasonably accurate values of total cloud absorption, with the higher spectral resolution of our model generally yielding slightly lower values than found by prior investigators. This may be an expected consequence of allowing the droplet absorption to vary spectrally within the water vapor absorption bands, but may also be due to our use of a more detailed treatment of water vapor transmission.

Our study of the dependence of total cloud absorption on the various input variables to our model indicates that cloud absorption depends strongly on both the column water vapor above the cloud top, which is largely a function of cloud top height and mixing ratio above the cloud, and on solar zenith angle. For a boundary layer cloud the absorption is typically 0.09 (expressed as a fraction of the extraterrestrial insolation) for overhead sun, but this value may almost double in the unlikely event that the water vapor is completely removed from above the cloud, and may be halved at solar zenith angles larger than about 70°. Effects of cloud temperature or droplet size distribution may typically perturb these values by $\pm$0.01, provided the cloud does not become very tenuous, in which case the absorption decreases to the clear sky limit.

Absorption by water vapor above the cloud top is usually sufficiently strong that the cloud droplets are the dominant absorbers of solar radiation within the cloud. Water vapor within the cloud may at times absorb very little of the incident solar radiation. In general, however, it cannot be neglected because its influence increases with decreasing vapor above the cloud until its contribution to the total cloud absorption may be comparable to the droplets.

The above results are moderately encouraging in terms of parameterizing the absorption of solar radiation in clouds for use by climate models. It appears that details of the cloud type and composition may not be too critical for such parameterizations. Provided the cloud is not very tenuous and there is a modest amount of water vapor above the cloud, the main dependence of cloud absorption is on solar zenith angle. Major difficulties are then identifying when the clouds are so thin that they fall below the asymptotic limit in absorption (Fig. 8), when their aspect ratios are sufficiently high that absorption is reduced due to side effects (Fig. 10), and when the water vapor amount above the cloud is sufficiently small that the cloud absorption increases sharply (Fig. 6). Many climate models keep the vertical distribution of water vapor as a prognostic variable, allowing this last effect to be parameterized explicitly.

Another encouraging result is found in the dependences of the total atmospheric absorption (i.e., cloud plus above-cloud absorption) on the various input variables. It appears that there may be a number of cloudy configurations for which the total atmospheric absorption depends very little on the details of cloud type, water vapor content and even solar zenith angle. This allows the potential for reasonably accurate estimates of the surface solar radiation budget from satellite measurements of reflected solar irradiance. The challenge will then rest in detecting exceptions to these configurations, which may include cases of tenuous clouds and partially cloud-filled fields of view.

Acknowledgment. Partial funding for this research from the National Aeronautics and Space Administration under Grants NAG 5-106 and NAG 5-101 is gratefully acknowledged.

REFERENCES

Appleby, J. F., and W. M. Irvine, 1973: Path-length distributions of photons diffusely reflected from a semi-infinite atmosphere. *Astrophys. J.*, **183**, 337–346.

Davies, R., 1978: The effect of finite geometry on the three-dimensional transfer of solar irradiance in clouds. *J. Atmos. Sci.*, **35**, 1712–1725.

Hale, G. M., and M. R. Querry, 1973: Optical constants of water in the 200-nm to 200-μm wavelength region. *Appl. Opt.*, **12**, 555–563.

Irvine, W. M., 1964: The formation of absorption bands and the distribution of photon optical paths in a scattering atmosphere. *Bull. Astron. Inst. Neth.*, **17**, 266–279.

Kargin, B. A., L. D. Krasnokutskaya and Ye. M. Feygel'son, 1972: Reflection and absorption of solar radiant energy by cloud layers. *Izv. Acad. Sci. USSR, Atmos. Ocean. Phys.*, **8**, 505–517.

King, M. D., 1981: A method for determining the single scattering albedo of clouds through observation of the internal scattered radiation field. *J. Atmos. Sci.*, **38**, 2031–2044.

Kneizys, F. X., E. P. Shettle, W. O. Gallery, J. H. Chetwynd, Jr., L. W. Abreu, J. E. A. Selby, R. W. Fenn and R. A. McClatchey, 1980: Atmospheric transmittance/radiance: Computer code LOWTRAN 5. AFGL-TR-80-0067, Air Force Geophysical Laboratories, Hanscomb AFB, MA, 233 pp.

Lacis, A. A., and J. E. Hansen, 1974: A parameterization for the absorption of solar radiation in the earth's atmosphere. *J. Atmos. Sci.*, **31**, 118–133.

Liou, K.-N., 1980: *An Introduction to Atmospheric Radiation.* Academic Press, 392 pp.

——, and T. Sasamori, 1975: On the transfer of solar radiation in aerosol atmospheres. *J. Atmos. Sci.*, **32**, 2166–2177.

——, and G. D. Wittman, 1979: Parameterization of the radiative properties of clouds. *J. Atmos. Sci.*, **36**, 1261–1273.

McClatchey, R. A., R. W. Fenn, J. E. A. Selby, F. E. Volz and J. S. Garing, 1972: Optical properties of the atmosphere, 3rd ed., AFCRL-72-0497, Air Force Cambridge Research Laboratories, Bedford, MA, 108 pp.

Paltridge, G. W., and C. M. R. Platt, 1976: *Radiative Processes in Meteorology and Climatology.* Elsevier, 318 pp.

Robertson, D. C., L. S. Bernstein, R. Haimes, J. Wunderlich and L. Vega, 1981: 5-cm^{-1} band model option to LOWTRAN 5. *Appl. Opt.*, **20**, 3218–3226.

Slingo, A., and H. M. Schrecker, 1982: On the shortwave radiative properties of stratiform water clouds. *Quart. J. Roy. Meteor. Soc.*, **108**, 407–426.

Stephens, G. L., 1978: Radiation profiles in extended water clouds. I: Theory. *J. Atmos. Sci.*, **35**, 2111–2122.

Thekaekara, M. P., and A. J. Drummond, 1971: Standard values for the solar constant and its spectral components. *Nature*, **229**, 6–9.

Twomey, S., and T. Cocks, 1982: Spectral reflectance of clouds in the near-infrared: Comparison of measurements and calculations. *J. Meteor. Soc. Japan*, **60**, 583–592.

van de Hulst, H. C., 1980: *Multiple Light Scattering.* Academic Press, 739 pp.

Welch, R. M., and S. K. Cox, 1980: The effect of monomodal drop size distributions, cloud top heights, cloud thickness and vertical water vapor profiles upon cloud heating rates and the cloud radiation field. *Solar Radiation and Clouds. Meteor. Monogr.*, No. 39, Amer. Meteor. Soc., 3–21.

Wiscombe, W. J., 1979: Mie scattering calculations: Advances in technique and fast, vector-speed computer codes. NCAR Tech. Note TN-140+STR, National Center for Atmospheric Research, Boulder, CO, 91 pp.

——, and J. W. Evans, 1977: Exponential-sum fitting of radiative transmission functions. *J. Comput. Phys.*, **24**, 416–444.